

Discrete source method for spectroscopic analysis of nano-particles on a plane interface

Elena Eremina¹, Yuri Eremin² and Thomas Wriedt¹

¹ Institut für Werkstofftechnik, Badgasteiner Strasse 3, 28359 Bremen, Germany

² Faculty of Applied Mathematics and Computer Science, Moscow State University, Lenin's Hills, 119992 Moscow, Russia

E-mail: eremina@iwt.uni-bremen.de and eremin@cs.msu.su

Received 2 June 2005, accepted for publication 13 September 2005

Published 21 October 2005

Online at stacks.iop.org/JOptA/7/706

Abstract

In this paper the discrete source method (DSM) is applied to analyse light scattering from nano-particles on a prism surface. Results of a comparison of an approximate Mie model and the rigorous DSM model, which accounts for the light scattering interaction of the particle with the prism surface, are presented. It is shown that taking into account the particle–prism interaction plays a significant role for a correct interpretation of spectroscopic measurements.

Keywords: light scattering, nano-particles, rigorous model

(Some figures in this article are in colour only in the electronic version)

1. Introduction

Nano-particle investigation plays an important role in many fields of science and technology. For example, PSL nano-particles are used for the calibration of surface scanners, which are used as silicon wafer inspection tools. Viruses are nanometre scale particles consisting of proteins and genetic materials. Cellular macromolecular complexes, which govern most cell functions, are typically in the range of a few tens of nanometres. Therefore, an accurate determination of the sizes of nano-scale objects will improve our understanding of their functioning and behaviour. Most approaches based on optical microscopy cannot be used for these purposes, mainly because the particle and structure sizes are smaller than the Rayleigh limit. There are several different approaches to handle this problem: the first one uses angle resolved scattering [1, 2]; the second one consists of spectrum measurements [3, 4].

The detection and sizing of nano-objects often involves some additional conditions. In virus detection the viruses are usually diluted in aqua; contaminating nano-particles in chip manufacturing are often situated in a layer on a substrate. In those cases taking into account the environment in scattering theory can play an important role for the proper detection of the objects size. One of the methods for the investigation

of light scattering by nano-particles which takes into account the complete light scattering interaction of an obstacle and layered medium is the discrete source method (DSM) [5]. In the present paper the DSM is applied to analyse the influence of the local environment on particle size detection. It has been found that the correct interpretation of measurement results might be in doubt without accounting for the particle–surface interaction. The paper is organized as follows: first the DSM theory is presented then the realization of the numerical algorithm is described. In the final part simulation results and discussion are given.

2. Discrete source method

Consider an axial symmetric penetrable particle with interior domain D_i and smooth boundary ∂D deposited above the plane interface Σ . We denote the prism domain by D_1 and the ambient domain exterior to the particle filled with water by D_0 . Let us introduce a Cartesian coordinate system $Oxyz$ by choosing its origin O at the intersection point of the axis of symmetry of the particle and the plane Σ . The Z -axis coincides with the axis of symmetry and is directed into domain D_0 , so that the plane $z = 0$ coincides with the Σ plane. We assume that the exciting field $\{\mathbf{E}^0, \mathbf{H}^0\}$ is a plane wave propagating

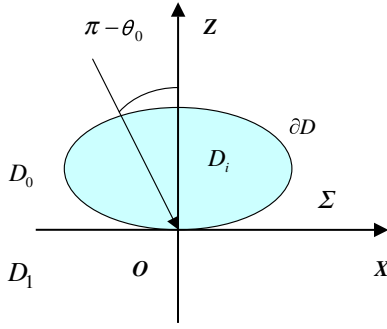


Figure 1. Problem geometry.

from the area D_0 at angle $\pi - \theta_0$ with respect to the Z -axis (figure 1). Then the mathematical statement of the scattering problem can be formulated in the following form:

$$\begin{aligned} \nabla \times \mathbf{H}_\zeta &= jk\varepsilon_\zeta \mathbf{E}_\zeta; & \nabla \times \mathbf{E}_\zeta &= -jk\mu_\zeta \mathbf{H}_\zeta \\ & \text{in } D_\zeta, \zeta = 0, 1, i, \\ \mathbf{n} \times (\mathbf{E}_i - \mathbf{E}_0) &= 0, & \mathbf{n} \times (\mathbf{H}_i - \mathbf{H}_0) &= 0, & \text{at } \partial D \\ \mathbf{e}_z \times (\mathbf{E}_0 - \mathbf{E}_1) &= 0, & \mathbf{e}_z \times (\mathbf{H}_0 - \mathbf{H}_1) &= 0, & \text{at } \Sigma \end{aligned} \quad (1)$$

and radiation (attenuation) conditions at infinity.

Here, \mathbf{n} is the outward unit normal vector to ∂D , $k = \omega/c$, ε and μ are the permittivity and permeability, \mathbf{e}_z is a unit normal to Σ , and $\{\mathbf{E}_\zeta, \mathbf{H}_\zeta\}$ stands for the total field in the corresponding domain D_ζ . Note that the total field in D_0 is a superposition of the exciting field and the scattered one, that is $\mathbf{E}_0 = \mathbf{E}_0^s + \mathbf{E}^0$, $\mathbf{H}_0 = \mathbf{H}_0^s + \mathbf{H}^0$. If $\text{Im } \varepsilon_\zeta, \mu_\zeta \leq 0$ (the time dependence for the fields is chosen as $\exp\{j\omega t\}$) and the particle surface is smooth enough, $\partial D \subset C^{(1,\omega)}$, then the above boundary-value problem is uniquely solvable.

An approximate solution to the scattering problem (1) is constructed to fulfil the transmission conditions on the plane interface Σ , taking into account the rotational symmetry of the scattering problem geometry (particle plus interface) and the polarization of the exciting field [5]. In the frame of the DSM the approximate solution is represented as a finite linear combination of the fields of dipoles and multipoles which analytically satisfy the transmission conditions enforced at the plane interface Σ . Then the approximate solution satisfies the Maxwell equations in the domains D_ζ , $\zeta = 0, 1, i$, infinity conditions and the transmission conditions at the interface Σ . Eventually, the scattering problem is reduced to the problem of approximating the exciting field on the particle surface ∂D . The amplitudes of discrete sources are determined from the boundary conditions at the particle surface, which can be rewritten as

$$\mathbf{n} \times (\mathbf{E}_i - \mathbf{E}_0^s) = \mathbf{n} \times \mathbf{E}^0, \quad \mathbf{n} \times (\mathbf{H}_i - \mathbf{H}_0^s) = \mathbf{n} \times \mathbf{H}^0 \quad \text{at } \partial D \quad (2)$$

where $\{\mathbf{E}^0, \mathbf{H}^0\}$ is a sum of incoming plane waves and those reflected from the interface.

To construct the approximate solution we will take into account the axial symmetry of the problem geometry and the polarization of the external excitation. In the case of P polarized light the exciting field accepts the following form:

$$\mathbf{E}^0 = (\mathbf{e}_x \cos \theta_0 + \mathbf{e}_z \sin \theta_0) \exp\{-jk_e(x \sin \theta_0 - z \cos \theta_0)\},$$

$$\mathbf{H}^0 = -\mathbf{e}_y n_0 \cos \theta_0 \exp\{-jk_e(x \sin \theta_0 - z \cos \theta_0)\},$$

where $k_e = k\sqrt{\varepsilon_e \mu_e}$.

Implementing plane wave resolution, one gets

$$\exp\{\pm j\nu \cos \varphi\} = \sum_{m=0}^{\infty} (2 - \delta_{0m})(\pm j)^m J_m(\nu) \cos m\varphi,$$

where J_m is the cylindrical Bessel function and δ_{0m} is a Kronecker symbol.

The Fourier harmonics for the external excitation in a cylindrical coordinate system can be written as

$$\begin{aligned} \mathbf{E}_m^0 &= \{\mathbf{E}_{m\rho}^{0,P}(\eta) \cos(m+1)\varphi; \mathbf{E}_{m\rho}^{0,P}(\eta) \sin(m+1)\varphi; \\ & \mathbf{E}_{mz}^{0,P}(\eta) \cos(m+1)\varphi\}, \\ \mathbf{H}_m^0 &= \{\mathbf{H}_{m\rho}^{0,P}(\eta) \sin(m+1)\varphi; \mathbf{H}_{m\rho}^{0,P}(\eta) \cos(m+1)\varphi; \\ & \mathbf{H}_{mz}^{0,P}(\eta) \sin(m+1)\varphi\}. \end{aligned}$$

Hence, to take the polarization of the external excitation into account we use some linear combination of electrical and magnetic multipoles, which are deposited along the axis of symmetry of the particle. For the scattered field representation outside a particle the following vector potentials are used:

$$\begin{aligned} \mathbf{A}_{mn}^{e,0}(\eta, z_n) &= \{G_m^e(\eta, z_n) \cos(m+1)\varphi; \\ & -G_m^e(\eta, z_n) \sin(m+1)\varphi; -g_{m+1}(\eta, z_n) \cos(m+1)\varphi\}, \\ \mathbf{A}_{mn}^{h,0}(\eta, z_n) &= \{G_m^h(\eta, z_n) \sin(m+1)\varphi; \\ & G_m^h(\eta, z_n) \cos(m+1)\varphi; -g_{m+1}(\eta, z_n) \sin(m+1)\varphi\}, \\ \mathbf{A}_{0n}^{e,h,0}(\eta, z_n) &= \{0; 0; G_0^{h,e}(\eta, z_n)\}. \end{aligned}$$

Here the corresponding azimuthal Fourier harmonics of the Green tensor components in D_0 can be presented as Weyl–Sommerfeld integrals [5]:

$$\begin{aligned} G_m^{e,h}(\eta, z_n) &= Y_m^0(\eta, z_n) \\ &+ \int_0^\infty J_m(\lambda\rho) v_{11}^{e,h}(\lambda, z_n) \exp\{-\eta_0 z\} \lambda^{1+m} \partial\lambda, \\ g_m(\eta, z_n) &= \int_0^\infty J_m(\lambda\rho) v_{31}(\lambda, z_n) \exp\{-\eta_0 z\} \lambda^{1+m} \partial\lambda. \end{aligned} \quad (3)$$

$$Y_m^0(\eta, z_n) = \frac{k_0}{i} h_m^{(2)}(k_0 R_{\eta z_n}) \left(\frac{k_0 \rho}{R_{\eta z_n}} \right)^m,$$

$$R_{\eta z_n}^2 = \rho^2 + (z - z_n)^2$$

where $h_m^{(2)}$ is a spherical Hankel function, point $\eta = (\rho, z)$ belongs to the semi-plane $\varphi = 0$, while $\{z_n\}_{n=1}^\infty$ is a dense set of discrete source points distributed over a segment $\Gamma_z^0 \in D_i$ at the axis of symmetry and $v_{11}^{e,h}(z, z_n, \lambda)$, $v_{31}(z, z_n, \lambda)$ are the corresponding spectral functions given by

$$\begin{aligned} v_{11}^e(\lambda, z_n) &= \frac{\mu_1 \eta_0 - \mu_0 \eta_1}{\mu_1 \eta_0 + \mu_0 \eta_1} \frac{1}{\eta_0} \exp\{-\eta_0 z_n\} \\ v_{11}^h(\lambda, z_n) &= \frac{\varepsilon_1 \eta_0 - \varepsilon_0 \eta_1}{\varepsilon_1 \eta_0 + \varepsilon_0 \eta_1} \frac{1}{\eta_0} \exp\{-\eta_0 z_n\}; \\ & z \geq 0, \quad z_n \geq 0 \\ v_{31}(\lambda, z_n) &= \frac{2(\mu_1 \varepsilon_1 - \mu_0 \varepsilon_0)}{(\mu_1 \eta_0 + \mu_0 \eta_1)(\varepsilon_1 \eta_0 + \varepsilon_0 \eta_1)} \exp\{-\eta_0 z_n\} \end{aligned}$$

where $\eta_\zeta^2 = \lambda^2 + k_\zeta^2$, $k_\zeta^2 = k^2 \varepsilon_\zeta \mu_\zeta$, $\zeta = 0, 1$.

The vector potentials for the field representation inside a particle have the form

$$\begin{aligned}\mathbf{A}_{mn}^{e,i}(\eta, z_n) &= \{J_m^i(\eta, z_n) \cos(m+1)\varphi; \\ &\quad -J_m^i(\eta, z_n) \sin(m+1)\varphi; 0\}, \\ \mathbf{A}_{mn}^{h,i}(\eta, z_n) &= \{J_m^i(\eta, z_n) \sin(m+1)\varphi; \\ &\quad J_m^i(\eta, z_n) \cos(m+1)\varphi; 0\}, \\ \mathbf{A}_{0n}^{e,h,i}(\eta, z_n) &= \{0; 0; J_0^i(\eta, z_n)\};\end{aligned}$$

where $J_m^i(\eta, z_n) = j_m(k_i R_{\eta z_n})(\rho/R_{\eta z_n})^m$; j_m are the spherical Bessel functions.

Now, we can represent the approximate solution to the scattering problem for the P -polarized excitation as

$$\begin{aligned}\mathbf{E}_N^\zeta &= \sum_{m=0}^M \sum_{n=1}^{N_m^\zeta} \left\{ p_{mn}^\zeta \frac{j}{k\varepsilon_\zeta \mu_\zeta} \nabla \times \nabla \times \mathbf{A}_{mn}^{e,\zeta} + q_{mn}^\zeta \frac{j}{\varepsilon_\zeta} \nabla \times \mathbf{A}_{mn}^{h,\zeta} \right\} \\ &\quad + \sum_{n=1}^{N_0^\zeta} r_n^\zeta \frac{j}{k\varepsilon_\zeta \mu_\zeta} \nabla \times \nabla \times \mathbf{A}_n^{e,\zeta};\end{aligned}\quad (4)$$

$$\mathbf{H}_N^\zeta = \frac{j}{k\mu} \nabla \times \mathbf{E}_N^\zeta, \quad \zeta = 0, i.$$

The last term in (4) is associated with vertical electric dipoles. Here, N is a complex index incorporating M and N_m^ζ . Let us emphasize that in the frame of the DSM, the scattered field $\{\mathbf{E}_N^\zeta, \mathbf{H}_N^\zeta\}$ in domains $D_{0,1}$ can be represented in terms of the unitary set of amplitudes $\{p_{mn}^0, q_{mn}^0, r_n^0\}$ after the transmission conditions at the interface Σ are satisfied through Green's tensor components (3) [5].

Consider S -polarization of the exciting plane wave. In this case the exciting field accepts the following form:

$$\mathbf{E}^0 = \mathbf{e}_y \cos \theta_0 \exp\{-jk_c(x \sin \theta_0 - z \cos \theta_0)\},$$

$$\mathbf{H}^0 = (\mathbf{e}_x \cos \theta_0 + \mathbf{e}_z \sin \theta_0) \eta_0 \exp\{-jk_c(x \sin \theta_0 - z \cos \theta_0)\}.$$

The Fourier harmonics for the external excitation can be written as

$$\begin{aligned}\mathbf{E}_m^0 &= \{\mathbf{E}_{m\rho}^{0,S}(\eta) \sin(m+1)\varphi; & \mathbf{E}_{m\rho}^{0,S}(\eta) \cos(m+1)\varphi; \\ & \mathbf{E}_{mz}^{0,S}(\eta) \sin(m+1)\varphi\}, \\ \mathbf{H}_m^0 &= \{\mathbf{H}_{m\rho}^{0,S}(\eta) \cos(m+1)\varphi; & \mathbf{H}_{m\rho}^{0,S}(\eta) \sin(m+1)\varphi; \\ & \mathbf{H}_{mz}^{0,S}(\eta) \cos(m+1)\varphi\}.\end{aligned}$$

We will use the following electric and magnetic potentials:

$$\begin{aligned}\mathbf{A}_{mn}^{e,0}(\eta, z_n) &= \{G_m^e(\eta, z_n) \sin(m+1)\varphi; \\ & \quad G_m^e(\eta, z_n) \cos(m+1)\varphi; -g_{m+1}(\eta, z_n) \sin(m+1)\varphi\}, \\ \mathbf{A}_{mn}^{h,0}(\eta, z_n) &= \{G_m^h(\eta, z_n) \cos(m+1)\varphi; \\ & \quad -G_m^h(\eta, z_n) \sin(m+1)\varphi; -g_{m+1}(\eta, z_n) \cos(m+1)\varphi\}, \\ \mathbf{A}_{0n}^{e,h,0}(\eta, z_n) &= \{0; 0; G_0^{h,e}(\eta, z_n)\}.\end{aligned}$$

The vector potentials for the fields inside the particle have a form

$$\begin{aligned}\mathbf{A}_{mn}^{e,i}(\eta, z_n) &= \{J_m^i(\eta, z_n) \sin(m+1)\varphi; \\ & \quad -J_m^i(\eta, z_n) \cos(m+1)\varphi; 0\}, \\ \mathbf{A}_{mn}^{h,i}(\eta, z_n) &= \{J_m^i(\eta, z_n) \cos(m+1)\varphi; \\ & \quad J_m^i(\eta, z_n) \sin(m+1)\varphi; 0\}, \\ \mathbf{A}_{0n}^{e,h,i}(\eta, z_n) &= \{0; 0; J_0^i(\eta, z_n)\}.\end{aligned}$$

So, for S -polarization the approximate solution accepts the following form:

$$\begin{aligned}\mathbf{E}_N^\zeta &= \sum_{m=0}^M \sum_{n=1}^{N_m^\zeta} \left\{ p_{mn}^\zeta \frac{j}{k\varepsilon_\zeta \mu_\zeta} \nabla \times \nabla \times \mathbf{A}_{mn}^{e,\zeta} + q_{mn}^\zeta \frac{j}{\varepsilon_\zeta} \nabla \times \mathbf{A}_{mn}^{h,\zeta} \right\} \\ &\quad + \sum_{n=1}^{N_0^\zeta} r_n^\zeta \frac{j}{k\varepsilon_\zeta \mu_\zeta} \nabla \times \nabla \times \mathbf{A}_n^{h,\zeta};\end{aligned}\quad (5)$$

$$\mathbf{H}_N^\zeta = \frac{j}{k\mu} \nabla \times \mathbf{E}_N^\zeta, \quad \zeta = 0, i.$$

The last term in (5) is associated with vertical magnetic dipoles [5]. The difference between (4) and (5) is caused by the fact that for S -polarization the vector \mathbf{H}^0 belongs to the incident plane.

The completeness of the system of lowest-order distributed multipoles used in (4) and (5) guarantees the convergence of the approximate solution to the exact one in any closed subset of D_0 [6].

As mentioned above the representations (4) and (5) satisfy all the conditions of the scattering problem (1) except the transmission conditions at the particle surface (2). These conditions are employed to determine amplitudes of discrete sources $\{p_{mn}^{0,i}, q_{mn}^{0,i}, r_n^{0,i}\}$. Since the scattering problem geometry is axially symmetric with respect to the Z -axis and discrete sources are distributed over the axis of symmetry, fulfilling the transmission conditions (2) at surface ∂D can be reduced to the sequential solution of the transmission problems for the Fourier harmonics of the fields. So, instead of matching the fields on the scattering surface, we can match their Fourier harmonics, thus reducing the approximation problem on the surface to a set of the problems enforced at the particle surface generatrix Im . By solving these problems one can determine the discrete source amplitudes $\{p_{mn}^{0,i}, q_{mn}^{0,i}, r_n^{0,i}\}$.

Various numerical schemes for the determination of the amplitudes are at our disposal. It has been found that stable results can be obtained by using the generalized point-matching technique and pseudo-solution of an over-determined system of linear equations. The DSM is a direct method and hence it allows solving the scattering problem for the entire set of incident angles θ_1 and both polarizations (P and S) at once. Besides that, the numerical scheme provides an opportunity to control the convergence of the approximate solution by posterior error estimation [5].

After the amplitudes of the discrete sources are determined, one can calculate the far field pattern $\mathbf{E}_\infty(\theta, \phi)$ of the scattered field, which is determined at the upper part of the unit semi-sphere $\Omega = \{0^\circ \leq \theta \leq 90^\circ, 0^\circ \leq \phi \leq 360^\circ\}$ and is given by

$$\begin{aligned}\mathbf{E}_\infty^s(\mathbf{r})/|\mathbf{E}^0(z=0)| &= \frac{\exp\{-jk_0 R\}}{R} \mathbf{E}_\infty(\theta, \phi) + O(R^{-2}), \\ R = |\mathbf{r}| \rightarrow \infty, \quad z > 0.\end{aligned}$$

We asymptotically estimate the Weyl-Sommerfeld integrals involved in (3) [5], which yields to the following representation for the θ, φ -components of the far field pattern corresponding

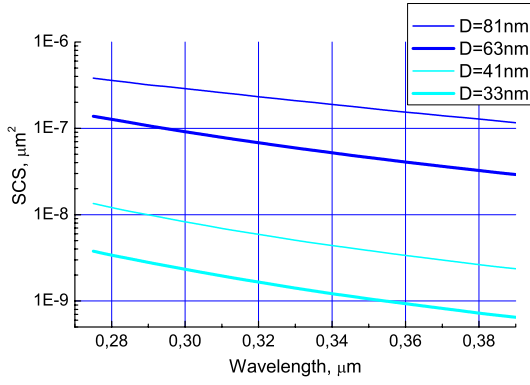


Figure 2. PSL sphere inside water layer on glass, incidence = 30°, DSM model.

to representation (4):

$$F_{\theta}^P(\theta, \varphi) = ik_0 \sum_{m=0}^M \cos(m+1)\varphi (ik_0 \sin \theta)^m \times \sum_{n=1}^{N_m^0} \{p_{mn}^0 [D_n^e \cos \theta + ik_0 \sin^2 \theta F_n] + q_{nm}^0 D_n^h\} - ik_0 \sin \theta \sum_{n=1}^{N_0^0} r_n^0 D_n^h \quad (6)$$

$$F_{\varphi}^P(\theta, \varphi) = -ik_0 \sum_{m=0}^M \sin(m+1)\varphi (ik_0 \sin \theta)^m \times \sum_{n=1}^{N_m^0} \{p_{mn}^0 D_n^e + q_{nm}^0 [D_n^h \cos \theta + ik_0 \sin^2 \theta F_n]\}$$

For S -polarized excitation following representation (5) one gets

$$F_{\theta}^S(\theta, \varphi) = ik_0 \sum_{m=0}^M \sin(m+1)\varphi (ik_0 \sin \theta)^m \times \sum_{n=1}^{N_m^0} \{p_{mn}^0 [D_n^e \cos \theta + ik_0 \sin^2 \theta F_n] - q_{nm}^0 D_n^h\},$$

$$F_{\varphi}^S(\theta, \varphi) = ik_0 \sum_{m=0}^M \cos(m+1)\varphi (ik_0 \sin \theta)^m \times \sum_{n=1}^{N_m^0} \{p_{mn}^0 D_n^e - q_{nm}^0 [D_n^h \cos \theta + ik_0 \sin^2 \theta F_n]\} + ik_0 \sin \theta \sum_{n=1}^{N_0^0} r_n^0 D_n^e, \quad (7)$$

where corresponding spectral functions $D_n^{e,h}$, F_n are

$$D_n^{e,h}(\theta) = \exp\{ik_0 z_n \cos \theta\} + ik_0 \cos \theta v_{11}^{e,h}(k_0 \sin \theta, z_n),$$

$$F_n(\theta) = ik_0 \cos \theta v_{31}(k_0 \sin \theta, z_n).$$

Hence, after the unknown amplitudes of discrete sources are determined, the far field pattern for P/S -

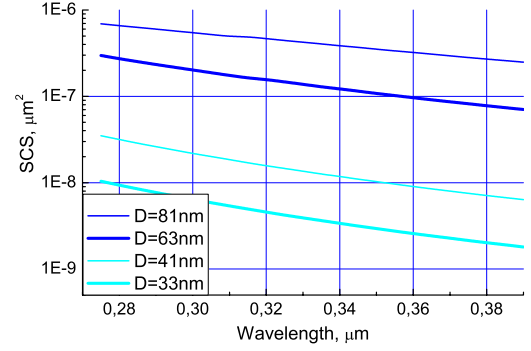


Figure 3. PSL sphere inside water, incidence = 30°, Mie model.

polarization (6), (7) is represented as finite linear combinations of elementary functions. This circumstance ensures economical computer analysis of the scattering characteristics in the wave zone.

The intensity of the scattered light will be considered as

$$I^{P,S}(\theta_1, \theta, \varphi) = |F_{\theta}^{P,S}(\theta_1, \theta, \varphi)|^2 + |F_{\varphi}^{P,S}(\theta_1, \theta, \varphi)|^2$$

where $F_{\theta,\varphi}^{P,S}(\theta_1, \theta, \varphi)$ are the components of the scattering diagram in a spherical coordinate system θ, φ for a P/S polarized incident wave. The scattered intensity of non-polarized light can be computed as

$$I(\theta_1, \theta, \varphi) = \frac{1}{2}(I^P(\theta_1, \theta, \varphi) + I^S(\theta_1, \theta, \varphi)). \quad (8)$$

We will also investigate the total scattering cross-section (SCS), which represents the summarized intensity, scattered into the upper half-space

$$\sigma_s(\theta_1) = \int_{\Omega} I(\theta_1, \theta, \varphi) d\omega, \quad (9)$$

where solid angle $\Omega = \{0 \leq \theta \leq 90^\circ; 0 \leq \varphi \leq 360^\circ\}$.

3. Results and discussion

In this section the numerical results obtained on the base of the DSM are presented. The main goal of our investigations was to clarify the influence of the local environment on the scattered light. PSL has been chosen as particle material. The ambient media is water and the prism material is glass. The refractive index data for PSL and for substrate have been taken from the public sources [7]. As wavelength range we took 250–400 nm in accordance with [4].

In figure 2 the results for the SCS for particles of different diameters deposited inside water on a glass substrate versus wavelength are presented. Figure 3 presents similar results for a Mie model for particles in water, without a prism. From figures 2 and 3 it is obvious that larger particles have a higher response.

Comparison results obtained for both models are presented in figures 4–7. In figure 4 particles with a diameter of 81 and 74 nm are chosen. The scattering response of even smaller particles, calculated by the Mie model (without taking into account the interface), is much higher than those

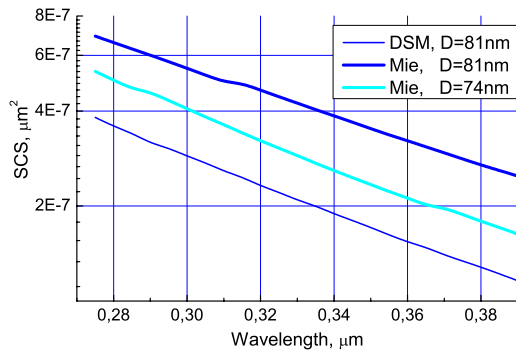


Figure 4. PSL sphere, DSM model against Mie model comparison.

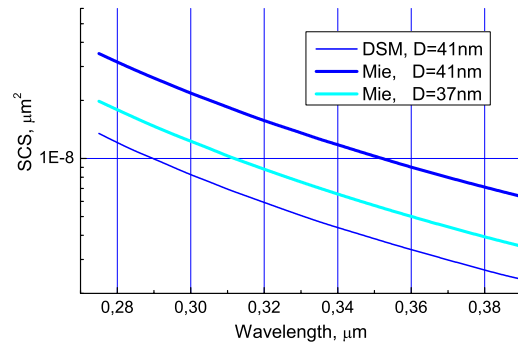


Figure 6. PSL sphere, DSM model against Mie model comparison.

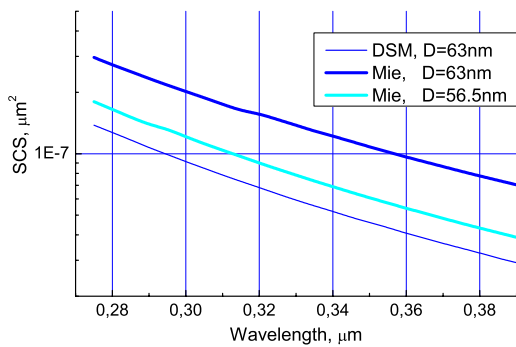


Figure 5. PSL sphere, DSM model against Mie model comparison.

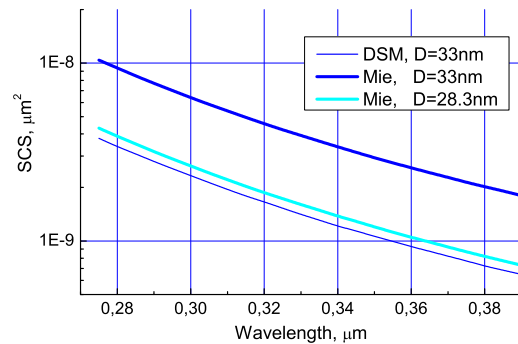


Figure 7. PSL sphere, DSM model against Mie model comparison.

calculated by the DSM. Similar results are presented in figure 5, but for particle diameters of 63 and 56.5 nm.

In figures 6 and 7 similar results for smaller particles are presented. We hope that the presented results allow clarification of the problem of experimental data interpretation in [3]. In particular, the difference in inclination of experimental and theoretical curves in [3] may be caused by the presence of an interface and not by a calculating error.

4. Conclusion

Based on the discrete source method, the numerical algorithm for analysis of the light scattering by nano-particles located inside water on a prism surface is presented. Results of the comparison of the Mie model (without taking into account the particle–interface interaction) and the rigorous DSM model are presented. It is shown that taking into account the

full environment plays a very important role for the correct interpretation of simulated and measured results.

Acknowledgments

We gratefully acknowledge funding of this research by Deutsche Forschungsgemeinschaft (DFG) and the Russian Foundation for Basic Research (RFBR).

References

- [1] Scheer C A and Stover J C 1999 *SPIE Proc.* **V3619** 72
- [2] Videen G et al 2005 *J. Quantum. Spectrosc. Radiat. Transfer* **93** 207
- [3] Chen K et al 2003 *Opt. Commun.* **228** 1
- [4] Raschke G et al 2004 *Nano Lett.* **4N10** 1853
- [5] Eremin Yu A 2000 *J. Commun. Technol. Electron.* **45** 269
- [6] Doicu A et al 2000 (London: Academic)
- [7] <http://swiss.csail.mit.edu/~jaffer/FreeSnell/>